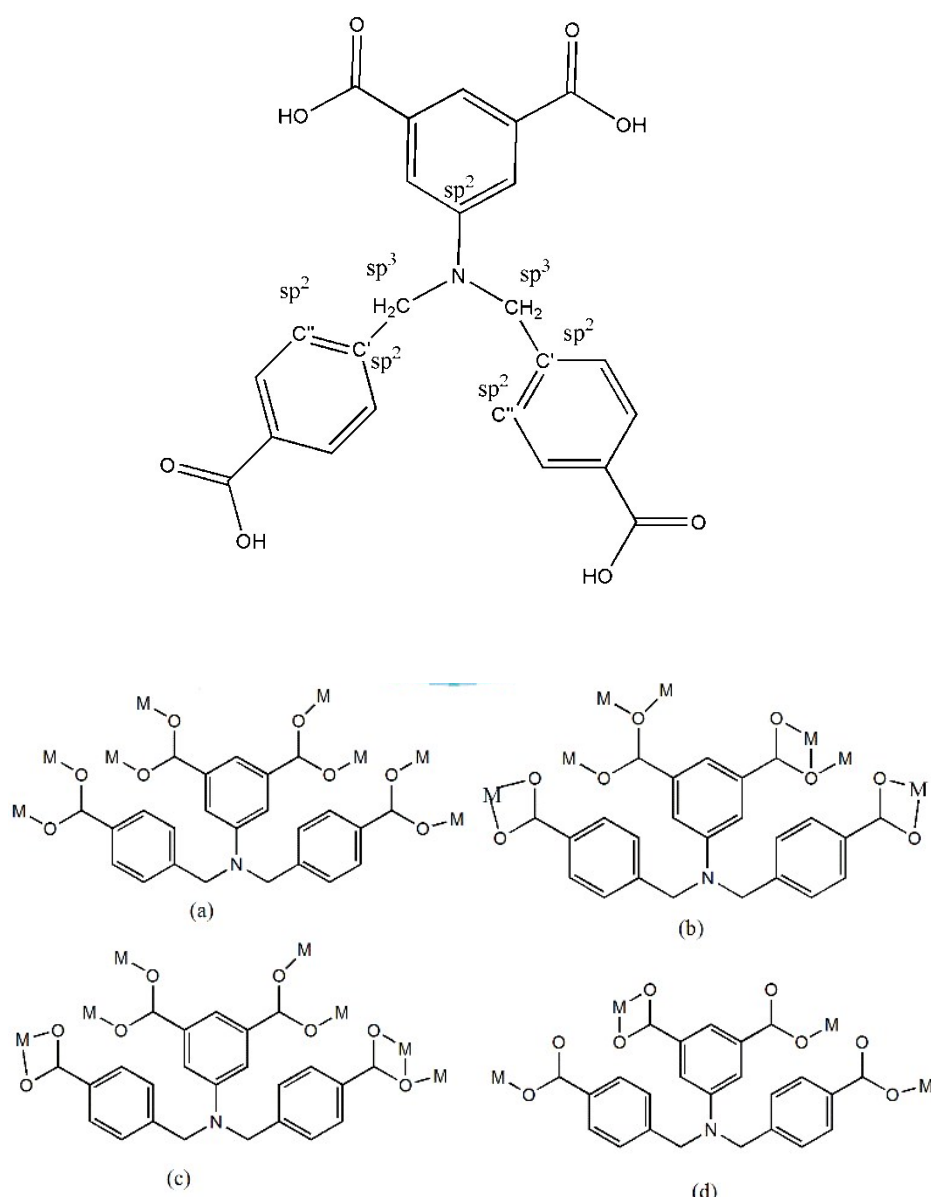


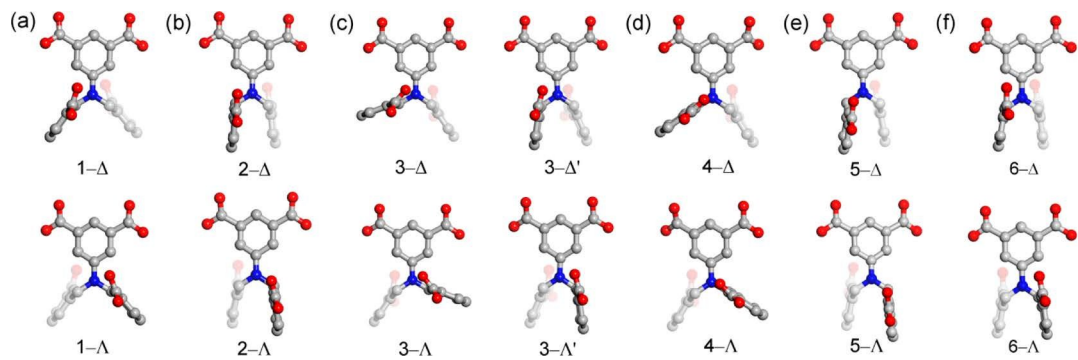
Supporting Information

Fluorescent sensing of nitro-aromatics by Zn(II) and Cd(II) based coordination polymers having 5-[bis(4-carboxybenzyl)-amino]isophthalic acid ligand

Lu Lu,^{a*} Jun Wang,^a Bin Xie,^a Jian-Qiang Liu,^{b*} Reena Yadav,^c Amita Singh,^c and Abhinav Kumar^{c*}



Scheme S1 The structural skeleton of 5-[bis(3-carboxybenzyl)-amino]isophthalic acid and its different coordination modes in this work.



Scheme S2 (a–f) Different stereoisomers of ligands existed in compounds in this work and was reported and found by Xing

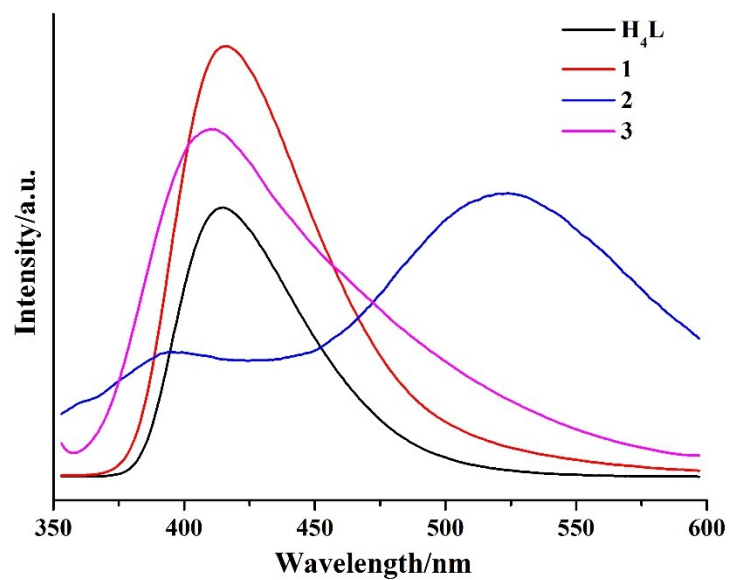


Fig. S1 view of PL at room temperature for H_4L ligand and **1-3**.

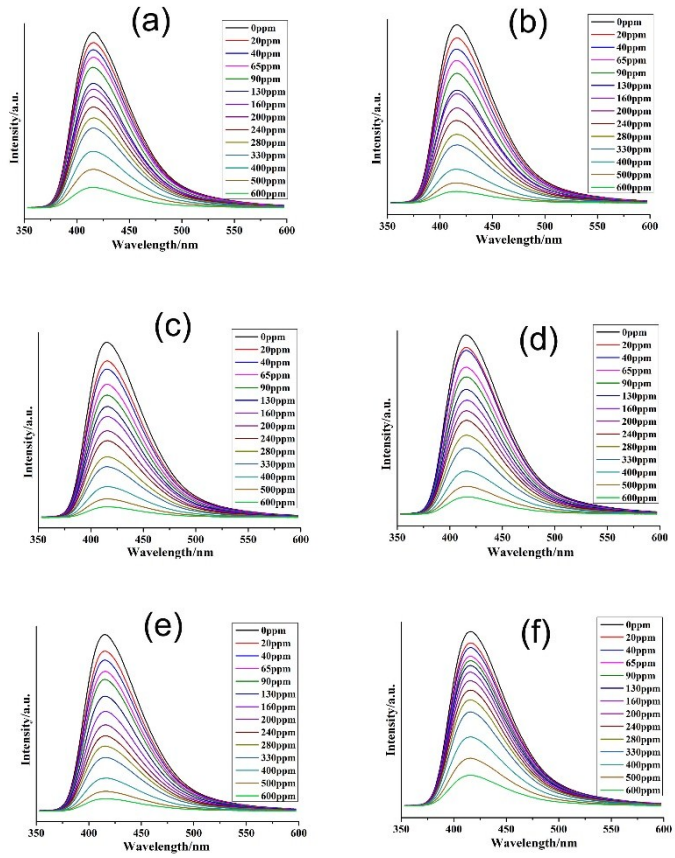


Fig. S2 Concentration-dependent luminescence quenching of **1** (dispersion in DMF) after adding different concentrations of (a) 1,3-DNB, (b) 2,4-DNT, (c) 2,6-DNT, (d) 2-NT, (e) 4-NT and (f) NB excited at 325 nm at room temperature.

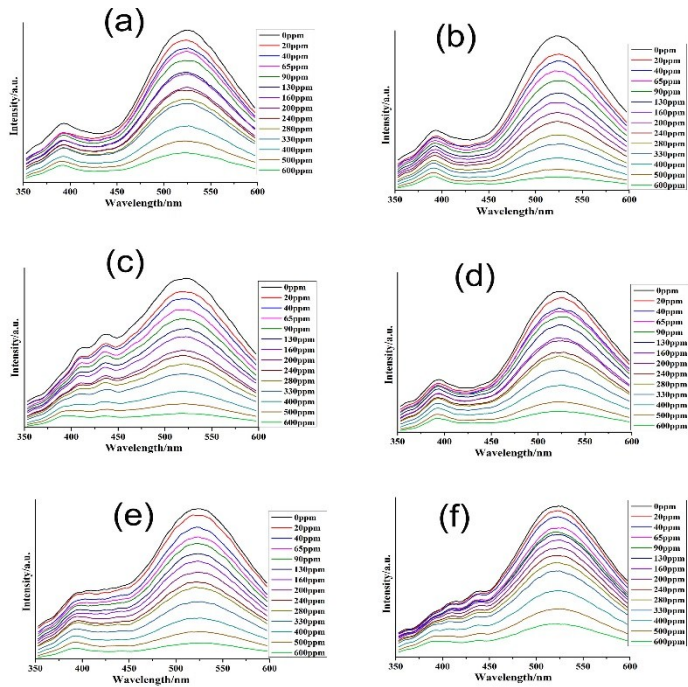


Fig. S3 Concentration-dependent luminescence quenching of **2** (dispersion in DMF) after adding different concentrations of (a) 1,3-DNB, (b) 2,4-DNT, (c) 2,6-DNT, (d) 2-NT, (e) 4-NT and (f) NB excited at 325 nm at room temperature.

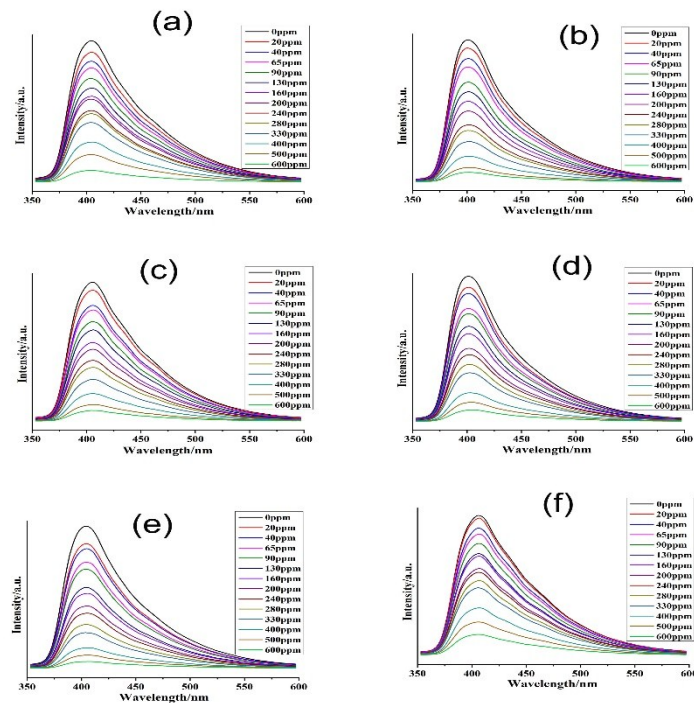


Fig. S4 Concentration-dependent luminescence quenching of **3** (dispersion in DMF) after adding different concentrations of (a) 1,3-DNB, (b) 2,4-DNT, (c) 2,6-DNT, (d) 2-NT, (e) 4-NT and (f) NB excited at 325 nm at room temperature.

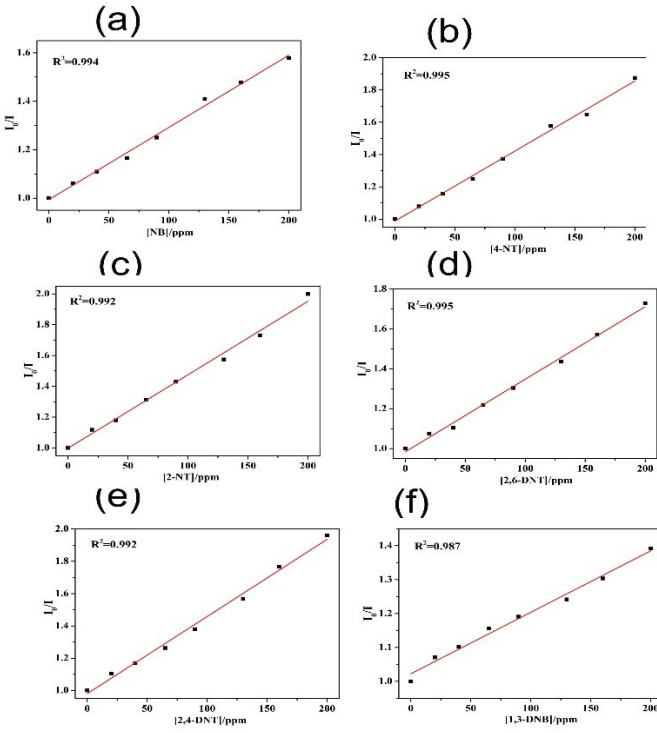


Fig. S5 plots of the I_0/I in **1**.

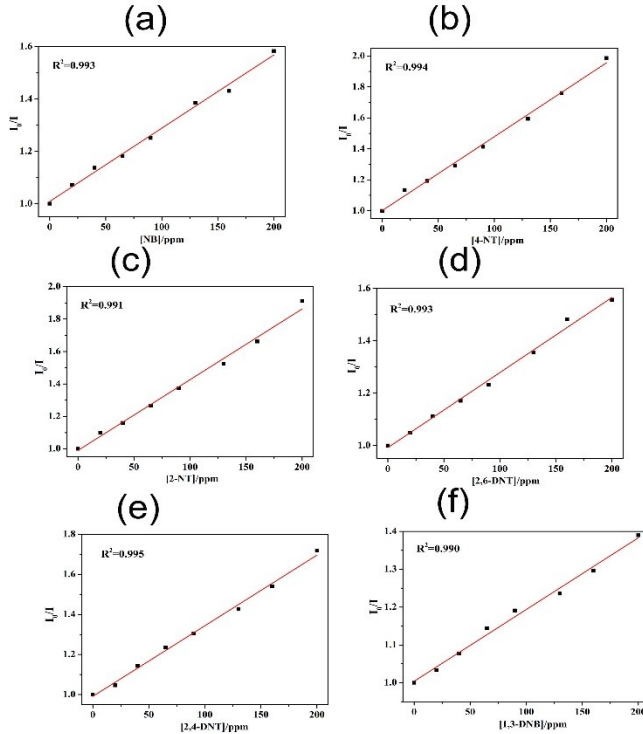


Fig. S6 plots of the I_0/I in **2**.

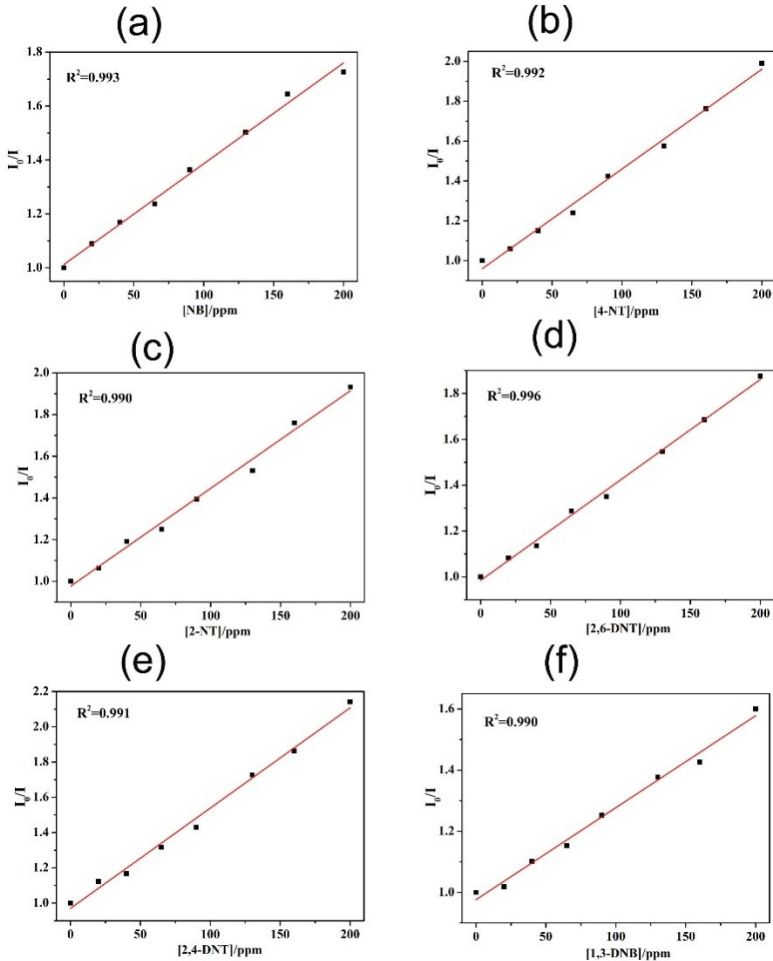


Fig. S7 plots of the I_0/I in **3**.

The asymmetric stretching vibration $\nu(\text{COO}^-)$ appear around 1610 cm^{-1} for **1-3**, and the symmetric stretching vibration $\nu(\text{COO}^-)$ are observed 1425 cm^{-1} for **1-3**. For these complexes, the difference between the asymmetric and symmetric stretches, $\Delta\nu_{\text{as}(\text{COO}^-)} - \nu_{\text{s}(\text{COO}^-)}$, are on the order of 150 cm^{-1} indicating that carboxyl groups are coordinated to the metal in a bidentate modes, consistent with the observed X-ray crystal structures of **1-3**. As shown in Fig. S8

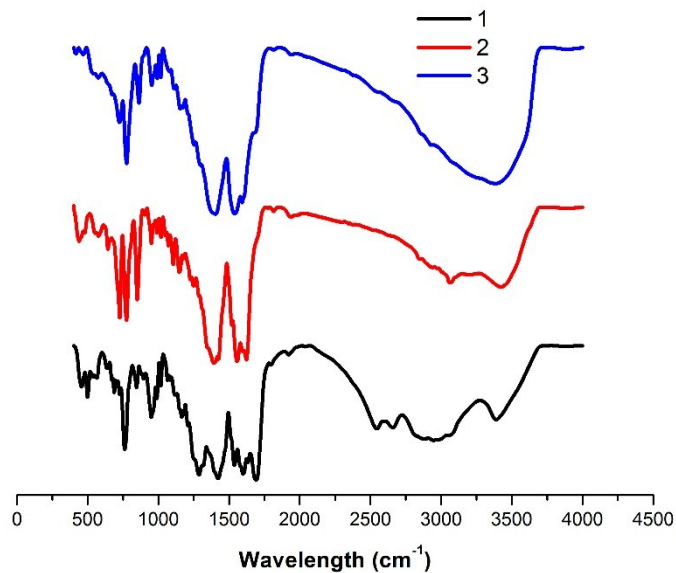


Fig. S8 view of the IR spectra in **1–3**.

Thermal gravimetric analyses (TGA) were carried out to examine the thermal stabilities of **1–3**. The results show that the weight of complexes **1–3** are very stable in air at ambient temperature, which make them potential candidates for practical applications. The samples were heated up in flowing N₂. For complex **1**, the decomposition of the compound occurs at ca. 330 °C. The remaining weight corresponds to the formation of ZnO. For **2**, the weight loss corresponding to the release of the coordinated and lattice water molecules is observed from 90 to 115 °C. The anhydrous complex begins to decompose at 360 °C. The TGA curve of **3** indicates that there is two loss steps. The first weight loss corresponds to the release of the one coordinated and one lattice water molecules is observed from 90 to 165 °C. Then a sharp weight-loss step was observed between 320 and 510°C, which can be attributed to the decomposition of organic ligands.

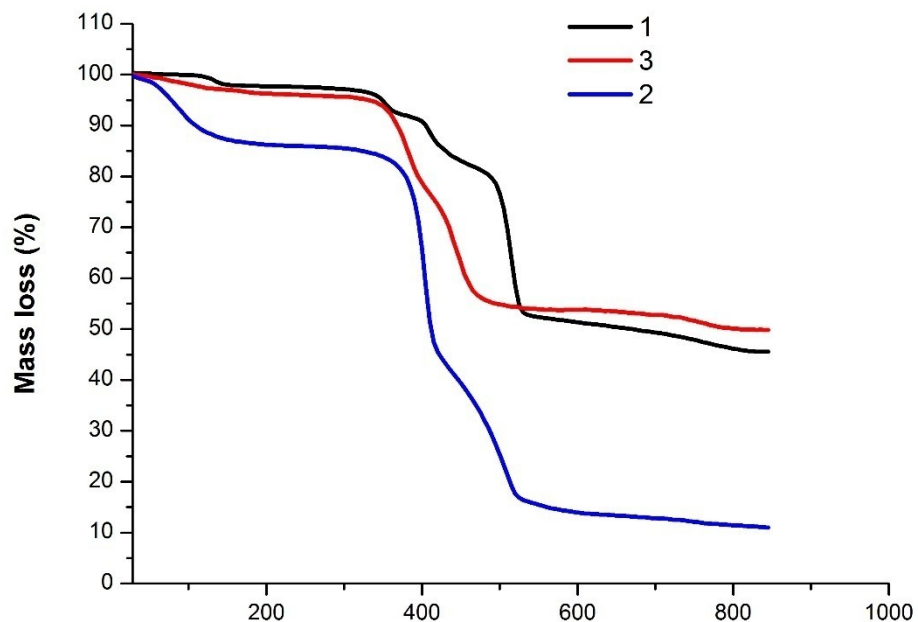


Fig. S9 View of the TGA in **1-3**.

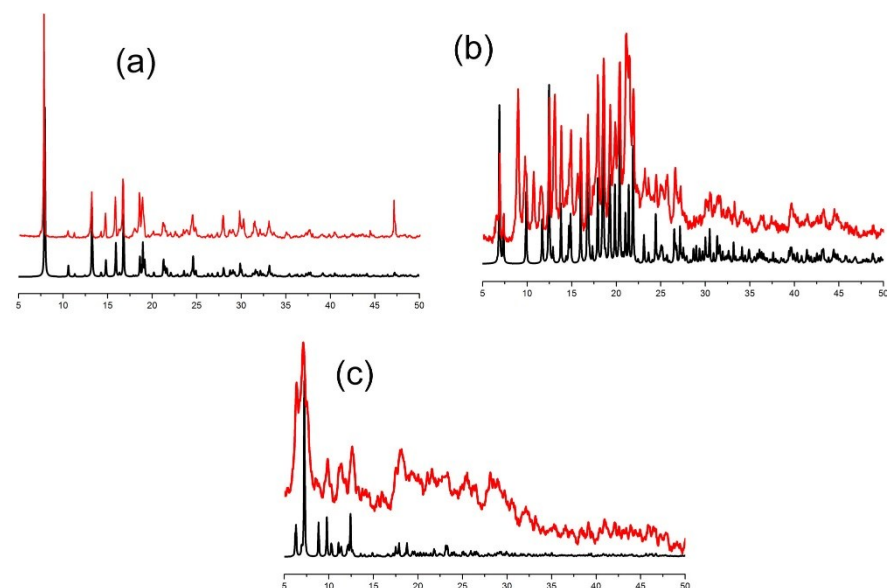
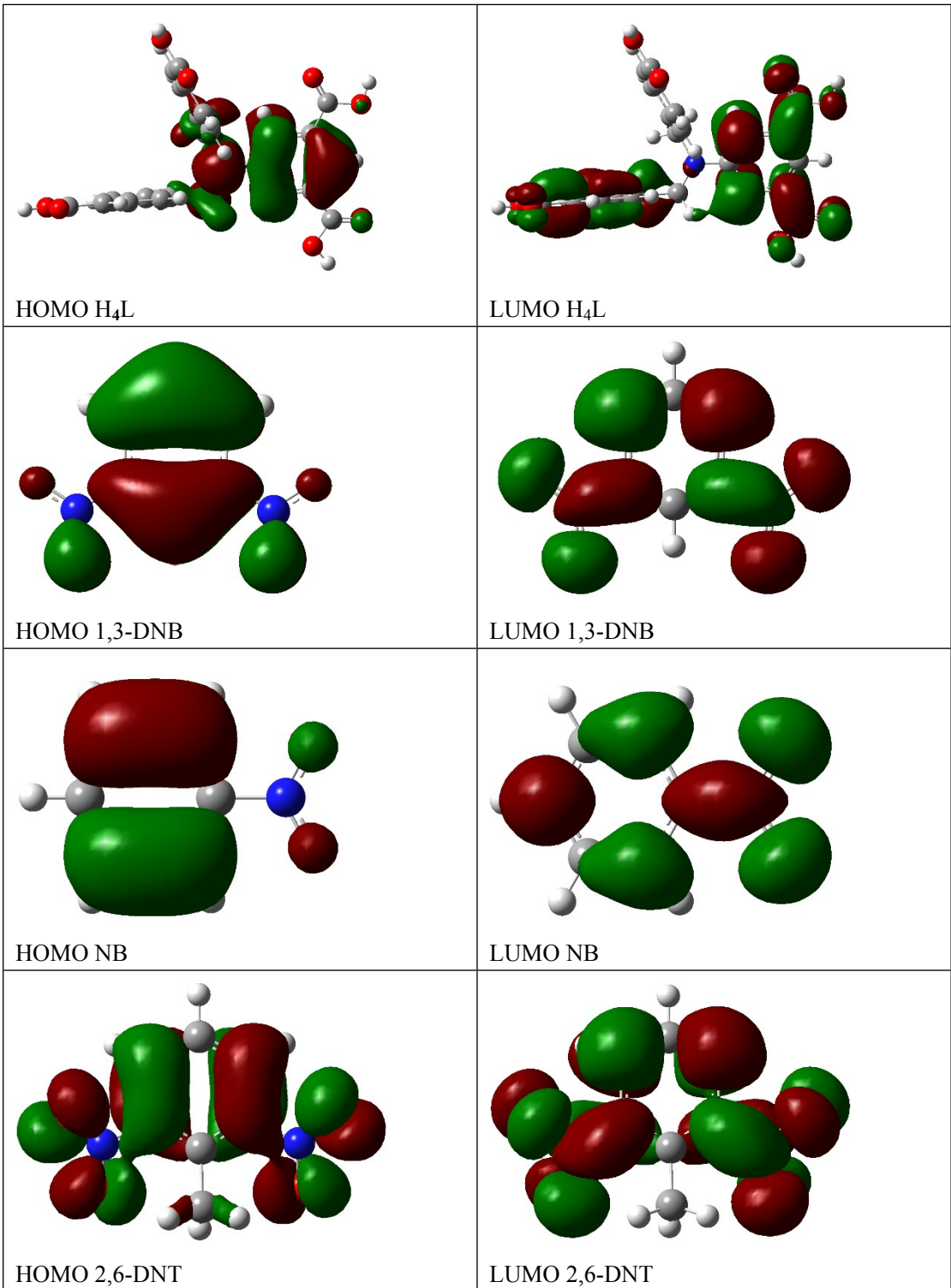


Fig. S10 The experimental X-ray powder diffraction diagrams of compounds **1-3** compared to the calculated ones.



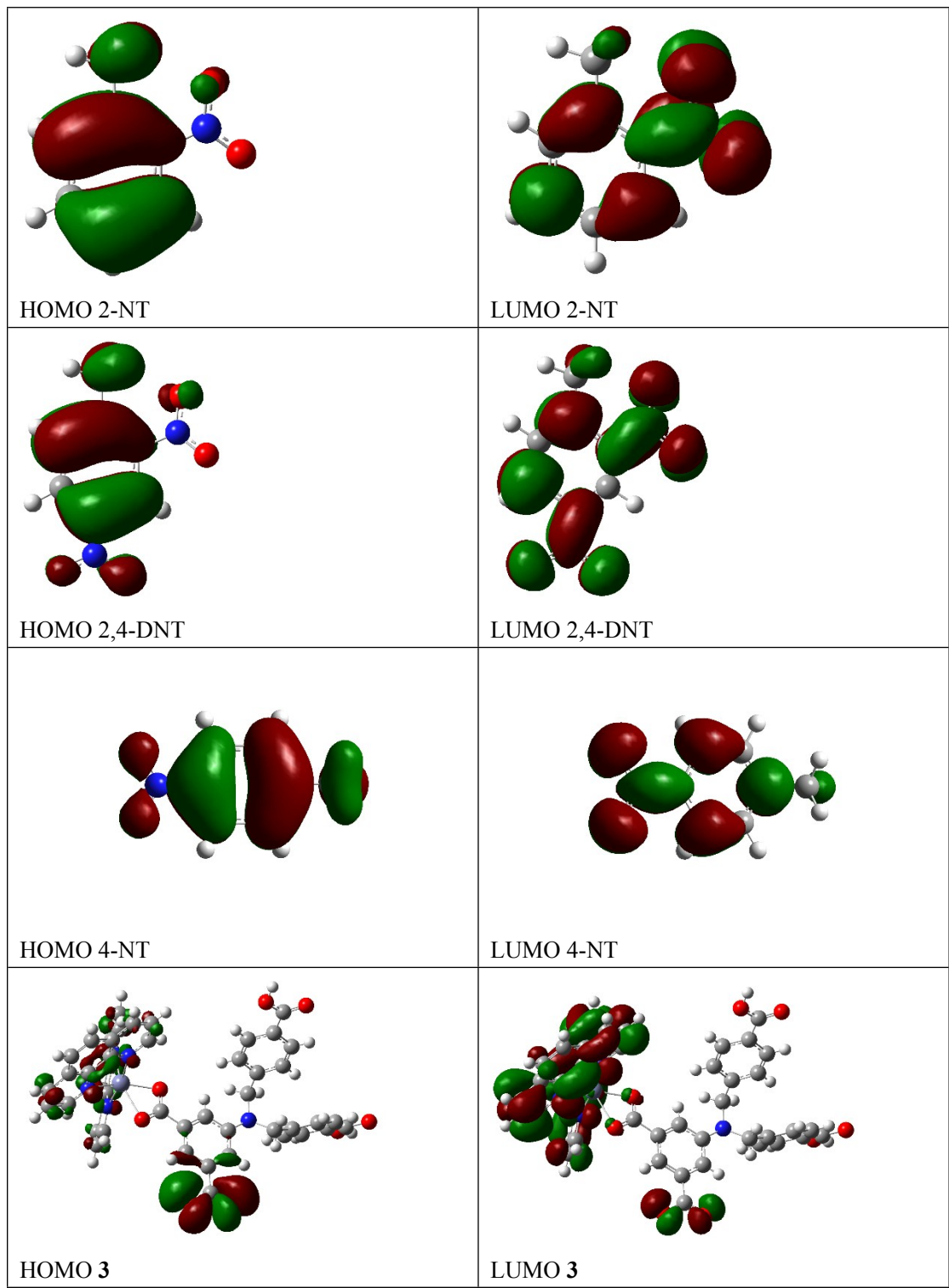


Fig. S11 HOMO-LUMO plots of nitro-aromatics

Table S1. Crystal data and structure refinement information for **1-3**

Parameter	1	2	3
Formula weight	576.11	1435.93	972.55
Crystal system	Monoclinic	Triclinic	Monoclinic
Space group	<i>P21/n</i>	<i>P-1</i>	<i>C/c</i>
Crystal color	Colorless	Colorless	Colorless
<i>a</i> , Å	9.6605(6)	14.9150(9)	25.448(15)
<i>b</i> , Å	22.2522(14)	15.7739(9)	15.151(8)
<i>c</i> , Å	11.3772(7)	16.0320(9)	11.157(7)
α , °	90	100.6592(7)	90
β , °	106.976(2)	112.2087(6)	108.613(10)
γ , °	90	107.2279(7)	90
<i>V</i> , Å ³	2339.2(3)	3141.7(3)	4077(4)
<i>Z</i>	4	2	4
ρ_{calcd} , g/cm ³	1.636	1.518	1.584
μ , mm ⁻¹	2.101	1.097	1.248
<i>F</i> (000)	1160	1416	1992
θ Range, deg	3.0-25.0	1.4-27.5	1.6-25.0
Reflection collected	4116	25158	6744
Independent reflections (<i>R</i> _{int})	0.064	0.020	0.0469
Reflections with <i>I</i> > 2σ(<i>I</i>)	3564	13366	5336
Number of parameters	316	688	586
<i>R</i> ₁ , <i>wR</i> ₂ (<i>I</i> > 2σ(<i>I</i>))*	0.0300, 0.0791	0.0587, 0.1633	0.0455, 0.0960
<i>R</i> ₁ , <i>wR</i> ₂ (all data)**	0.0374, 0.0823	0.0721, 0.1778	0.0668, 0.1235

* $R = \sum(F_o - F_c)/\sum(F_o)$, ** $wR_2 = \{\sum[w(F_o^2 - F_c^2)^2]/\sum(F_o^2)^2\}^{1/2}$.

Table S2. Selected bond distances (Å) and angles (deg) for **1-3**

Bond	<i>d</i> , Å	Bond	<i>d</i> , Å
------	--------------	------	--------------

	1		
Zn(1)-O(5)	1.944(2)	Zn(1)-O(4) ^b	1.919(2)
Zn(1)-O(6) ^e	1.9412(19)	Zn(1)-O(2) ^h	1.9404(19)
Zn(2)-O(8)	1.9339(19)	Zn(2)-O(3) ^a	1.923(2)
Zn(2)-O(7) ^f	1.9247(19)	Zn(2)-O(1) ^g	1.924(2)
	2		
Cd(1)-O(1)	2.553(5)	Cd(1)-O(9)	2.305(5)
Cd(1)-O(5) ^a	2.477(7)	Cd(1)-O(6) ^a	2.341(7)
Cd(1)-O(15) ^e	2.380(5)	Cd(1)-O(16) ^e	2.476(5)
Cd(1)-O(3) ^g	2.277(5)	Cd(1)-O(4) ^g	2.675(4)
Cd(2)-O(1)	2.408(5)	Cd(2)-O(1W)	2.496(8)
Cd(2)-O(9)	2.345(5)	Cd(2)-O(13) ^d	2.340(16)
Cd(2)-O(16) ^e	2.362(4)	Cd(2)-O(11) ^f	2.253(5)
Cd(3)-O(2)	2.213(5)	Cd(3)-O(10)	2.230(5)
Cd(3)-O(7) ^c	2.40 (2)	Cd(3)-O(8) ^c	2.298(17)
Cd(3)-O(12) ^f	2.314(5)	Cd(3)-O(4) ^g	2.309(5)
	3		
Zn(1)-O(2)	2.318(8)	Zn(1)-N(1)	2.141(8)
Zn(1)-N(2)	2.136(10)	Zn(1)-N(3)	2.127(8)
Zn(1)-N(4)	2.146(8)	Zn(1)-O(1)	2.112(7)
Zn(2)-O(3)	1.950(8)	Zn(2)-O(7) ^b	1.955(7)
Zn(2)-O(6) ^c	1.928(8)	Zn(2)-O(1W)	1.976(8)

Angle	ω , deg	Angle	ω , deg
1		1	
O(4) ^b -Zn(1)-O(5)	117.68(9)	O(5)-Zn(1)-O(6) ^e	110.04(8)
O(2) ^h -Zn(1)-O(5)	98.88(8)	O(4) ^b -Zn(1)-O(6) ^e	100.79(8)
O(2) ^h -Zn(1)-O(4) ^b	124.94(8)	O(2) ^h -Zn(1)-O(6) ^e	103.49(8)
O(3) ^a -Zn(2)-O(8)	106.00(8)	O(7) ^f -Zn(2)-O(8)	123.91(8)
O(1) ^g -Zn(2)-O(8)	100.25(9)	O(3) ^a -Zn(2)-O(7) ^f	99.25(8)
O(1) ^g -Zn(2)-O(3) ^a	124.63(9)	O(1) ^g -Zn(2)-O(7) ^f	105.02(8)
2		2	
O(1)-Cd(1)-O(9)	74.71(16)	O(1)-Cd(1)-O(5) ^a	140.59(19)
O(1)-Cd(1)-O(6) ^a	159.48(19)	O(1)-Cd(1)-O(15) ^e	80.67(17)
O(1)-Cd(1)-O(16) ^e	69.18(15)	O(1)-Cd(1)-O(3) ^g	82.45(16)
O(5) ^a -Cd(1)-O(9)	79.4(2)	O(6) ^a -Cd(1)-O(9)	99.9(2)
O(9)-Cd(1)-O(15) ^e	124.70(16)	O(3) ^g -Cd(1)-O(9)	131.28(15)
O(4) ^g -Cd(1)-O(9)	80.17(15)	O(5) ^a -Cd(1)-O(16) ^e	128.54(19)
O(1)-Cd(2)-O(1W)	143.6(2)	O(1)-Cd(2)-O(9)	76.83(17)
O(1W)-Cd(2)-O(9)	84.8(2)	O(1W)-Cd(2)-O(13) ^d	121.7(4)
O(1W)-Cd(2)-O(16) ^e	71.0(2)	O(9)-Cd(2)-O(11) ^f	83.06(19)
O(9)-Cd(2)-O(13) ^d	148.0(3)	O(9)-Cd(2)-O(16) ^e	72.63(16)
O(2)-Cd(3)-O(10)	146.09(16)	O(2)-Cd(3)-O(7) ^c	79.9(6)
O(2)-Cd(3)-O(8) ^c	126.9(4)	O(2)-Cd(3)-O(12) ^f	85.6(2)

O(7) ^c -Cd(3)-O(10)	132.5(6)	O(8) ^c -Cd(3)-O(10)	86.5(4)
O(10)-Cd(3)-O(12) ^f	84.5(2)	O(4) ^g -Cd(3)-O(10)	82.93(17)
O(7) ^c -Cd(3)-O(12) ^f	90.6(5)	O(4) ^g -Cd(3)-O(7) ^c	125.1(5)
		3	
O(1)-Zn(1)-O(2)	59.5(2)	O(1)-Zn(1)-N(1)	151.9(3)
O(1)-Zn(1)-N(2)	95.0(3)	O(1)-Zn(1)-N(3)	94.1(3)
O(1)-Zn(1)-N(4)	92.6(3)	O(2)-Zn(1)-N(1)	94.8(3)
O(2)-Zn(1)-N(2)	101.8(3)	O(2)-Zn(1)-N(3)	149.3(3)
O(2)-Zn(1)-N(4)	87.0(3)	N(1)-Zn(1)-N(2)	78.3(3)
N(1)-Zn(1)-N(3)	113.6(3)	N(1)-Zn(1)-N(4)	97.5(3)
N(2)-Zn(1)-N(3)	95.5(3)	N(2)-Zn(1)-N(4)	170.5(2)
O(1W)-Zn(2)-O(3)	112.7(4)	O(1W)-Zn(2)-O(7) ^b	95.4(3)
O(1W)-Zn(2)-O(6) ^c	116.4(4)	O(3)-Zn(2)-O(7) ^b	105.6(3)
O(3)-Zn(2)-O(6) ^c	107.4(3)	O(6) ^c -Zn(2)-O(7) ^b	118.7(3)

1: a= -3/2-x,-1/2+y, 1/2-z; b = -3/2-x,-1/2+y, 3/2-z; e = -2-x,-y, 1-z; f = -1-x,-y,-z; g = -1/2+x,1/2-y,-1/2+z; h= -1/2+x,1/2-y,1/2+z

2: a = -1+x,y,z; c = x,y, 1+z; d = 1+x,y,z; e = 1-x,1-y,1-z; f=1-x,1-y, 2-z; g = 2-x, 2-y,2-z

3: b = x,1+y,z; c = -1/2+x,3/2-y,-1/2+z

Table S3. The HOMO-LUMO energies for different analytes other than nitroaromatics.

Analyte	HOMO	LUMO
Nitrobenzene	-7.60	-2.44
Chloroform	-8.60	-1.36
Dichloromethane	-8.42	-0.44
Acetone	-6.64	-0.3
DMF	-6.32	0.99
Acetonitrile	-8.87	1.00
DMSO	-6.05	1.16
Water	-7.94	1.78
iso-propanol	-7.10	2.00
Methanol	-7.21	2.10
THF	-4.20	2.17
DMA	-5.85	2.37
Dioxane	-6.41	2.59